Role of electron injection in polyfluorene-based light emitting diodes containing PEDOT:PSS

Paul J. Brewer,[1] Paul A. Lane,[2] Jingsong Huang,[3] Andrew J. deMello,[1] Donal D. C. Bradley,[3] and John C. deMello[1,*]
[1]*Department of Chemistry, Imperial College London, London SW7 2AZ, United Kingdom*
[2]*Naval Research Laboratory, Washington, D.C., USA*
[3]*Blackett Laboratory, Imperial College London, London SW7 2BZ, United Kingdom*
(Received 21 October 2004; revised manuscript received 14 February 2005; published 25 May 2005)

We report electromodulation (EM) studies of polyfluorene-based light-emitting diodes containing poly(3,4-ethylene-dioxythiophene)-poly(styrene-sulfonate) (PEDOT:PSS), in which the barrier to hole injection is large ($\sim$0.7 eV). Measurements are reported on devices fabricated with aluminium and barium cathodes to provide respectively poor and efficient electron injection into the active layer. The Al devices exhibit low currents, indicating low rates of electron and hole injection, whereas the Ba devices exhibit high currents and high electroluminescence efficiencies, implying efficient injection of both electrons *and* holes despite the large hole injection barrier. The Al devices show conventional field-induced EM behavior consistent with the Stark effect (SE). The Ba devices show conventional SE behavior for low applied biases but, above turn-on, the (field-induced) SE features vanish, indicating suppression of the internal field, and are replaced by charge-induced bleaching and absorption features. The behavior of the devices is attributed to the presence of electron traps close to the PEDOT:PSS/organic interface. The experimental findings are consistent with earlier findings by Murata *et al.*, Van Woudenbergh *et al.*, Poplavskyy *et al.*, and Lane *et al.*

DOI: 10.1103/PhysRevB.71.205209 PACS number(s): 78.20.Jq

I. INTRODUCTION

Semiconducting polymers are of scientific and commercial interest owing to their applications in optoelectronic devices such as light-emitting diodes, solar cells and thin-film transistors.[1] There has been significant progress in the development of polymer devices in recent years with, for example, polymer light-emitting diodes (LEDs) now entering the market place as viable contenders to liquid crystal displays. To some extent, however, attempts to optimize the efficiencies and performance of polymer LEDs have been hindered by the relative absence of detailed models describing device operation. The fundamental processes governing device characteristics are the subject of debate and there is considerable interest in experimental measurements that provide insight into device operation.

In recent studies,[2–4] we used electromodulation (EM) spectroscopy to investigate the strength of the internal electric field in polyfluorene-based operational light-emitting diodes. These measurements indicated that, for many polymer LEDs under light emission conditions, screening effects by injected charge carriers lead to near-complete cancellation of the internal field. In the absence of a sizeable bulk field—and hence drift current—carrier transport is mediated primarily by diffusion in a manner similar to light-emitting electrochemical cells.[5] In order to screen the bulk semiconductor from the external field, the injected charges must accumulate at the counter electrode, and we therefore concluded that the observed field screening was due to either trapped electrons at the anode or trapped holes at the cathode. In separate studies Murata *et al.*,[6] Van Woudenbergh *et al.*,[7] and Poplavskyy *et al.*[8] had previously found evidence for electron accumulation close to the hole-injecting contact using devices based on poly(9,9-dioctylfluorene-alt-benzothiadiazole) [F8BT], a dialkoxy-p-phenylenevinylene [OC_1C_{10}-PPV], and poly(9,9-dioctylfluorene) [PFO] respectively. They found that hole-only devices show low currents whereas double-carrier devices show high currents and high efficiencies—implying that the presence of electrons in the device enhances hole injection. They attributed this to electron accumulation close to the anode, leading to an enhancement in the local electric field and a consequent improvement in hole injection. Poplavskyy *et al.* showed via a combination of current-voltage-luminance, dark injection transient current, time-of-flight photocurrent, and impedance spectroscopy measurements that the high current regime is reached via a transitionary regime in which an additional interfacial impedance component is generated at the anode and the contact becomes Ohmic.[8,9] The switching effect requires a cathode capable of injecting electrons. Most recently, Van Woudenbergh *et al.* have also published a study of PFO devices that confirmed the findings of Poplavskyy *et al.* and additionally demonstrated an important role for the detailed chemical structure of the PFO polymer, specifically the choice of end groups.[10]

The degree of field-redistribution assumed by Murata *et al.*[6] and Van Woudenbergh *et al.*[7] was relatively small, causing only a modest reduction in the bulk field-strength compared with the complete screening observed in our devices. However, given the similarity in device structure, in our previous manuscripts[2–4] we tentatively proposed that electron accumulation at the PEDOT:PSS/polyfluorene interface was also responsible for screening in our devices [see Fig. 1(a)]. Unfortunately, we were not able to test this assumption directly at the time since our measurements were performed on commercially sourced LEDs of a fixed structure.[11] In this work, by fabricating in-house two device types in which the cathode is selected to provide either efficient (Ba) or inefficient (Al) electron injection, we sought to test our earlier postulate that trapped electrons are responsible for the screening effect.

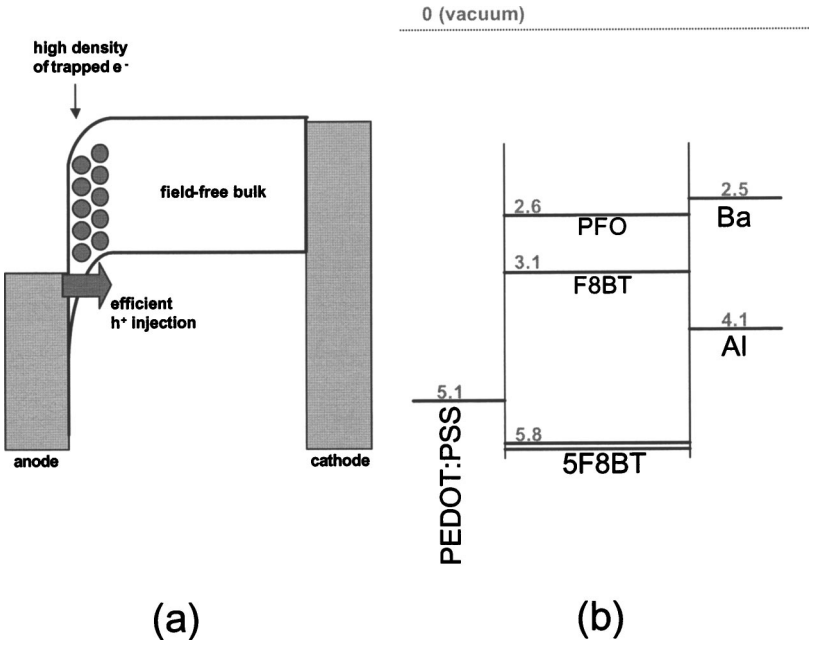

FIG. 1. (a) Schematic diagram showing the HOMO and LUMO energy levels in a trap-rich LED containing a high density of trapped electrons close to the anode; the charge accumulation at the anode causes local enhancement of the electric field, leading to an increased rate of hole injection, better balance between electron and hole currents, and higher overall device efficiencies. (b) Energy level diagram for an ITO/PEDOT:PSS/5BTF8/cathode device, where the cathode material is chosen to be either Al (Ref. 29) or Ba (Ref. 29) in order to achieve poor or efficient electron injection. The work function of the ITO/PEDOT:PSS anode is taken from Ref. 30.

II. RESULTS AND DISCUSSION

Devices were fabricated by successively coating an indium tin oxide anode with 80 nm thick layers of poly(3,4-ethylenedioxythiophene)-poly(styrene-sulfonate) (PEDOT:PSS) and a polymer blend containing 5% by weight poly(9,9-dioctylfluorene-*alt*-benzothiadiazole) (F8BT) and 95% poly(9,9-dioctylfluorene) (PFO). This blend is referred to as 5BTF8 and has previously been characterized as an effective material for green light-emitting resonant cavity and small area pulsed LEDs.[12] The active layer was then capped with 100 nm of either Ba or Al and the completed device was encapsulated in a nitrogen atmosphere glove-box. Current-voltage-luminance measurements were recorded with a Keithley 6517a electrometer.

Figure 1(b) shows approximate values for the work functions of PEDOT:PSS, Ba and Al and for the HOMO and LUMO energies of F8BT and PFO.[13,14] The HOMO levels of F8BT and PFO are approximately coincident ($\sim 5.8 \pm 0.1$ eV), and therefore similar hole injection barriers of 0.7 ± 0.2 eV exist for the two materials at the PEDOT:PSS/5BTF8 interface. This barrier height is relatively large and ordinarily one would expect only weak hole injection for typical drive voltages (<8 V). The LUMO of F8BT lies well below that of PFO so for an Al cathode electron injection will occur preferentially into F8BT subject to an approximate barrier height of 1.0 ± 0.2 eV. The Fermi level of Ba lies 0.6 ± 0.1 eV above the LUMO of F8BT and will therefore form an Ohmic contact with F8BT.[15] Hence, on the basis of simple energy considerations, we would expect Al devices to show low currents (due to poor electron and hole injection) and Ba devices to show high currents (due to good electron injection) but low efficiencies (due to poor hole injection). The observed behavior of Ba devices, however, did not match this simple model as we describe below.

Figure 2 shows the bias dependence of the current and luminance for typical Al and Ba devices. A delay of 10 s between initial application of the step-voltage and each measurement was employed to allow reasonable time for steady-state to be achieved. A striking feature of both devices is the symmetry of the current-voltage characteristics in the range -2 to $+2$ V. The injection of charge into a semiconductor is highly sensitive to interfacial barrier heights and in general strong rectification is expected for dissimilar electrode materials. The symmetric current-voltage characteristics are attributed to the presence of small quantities of conducting filaments in the active layer that act as shorts between the electrodes. These filaments dominate the current-voltage characteristics at low applied biases (since the rate of carrier

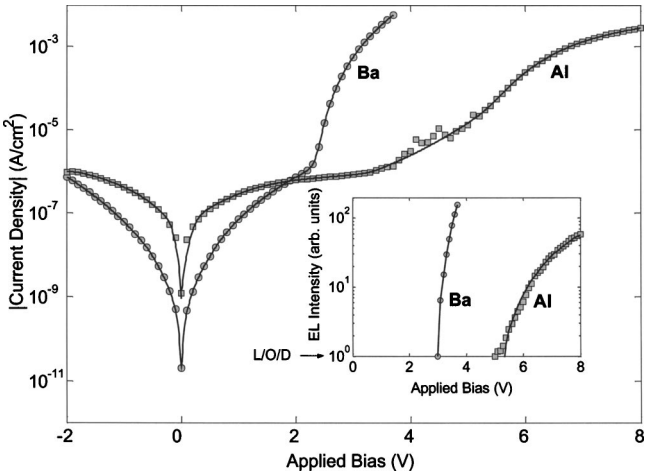

FIG. 2. Current-voltage-luminance measurements for devices based on ITO/PEDOT:PSS/5BTF8/Ba (circles) and ITO/PEDOT:PSS/5BTF8/Al (squares). The symmetrical *I-V* characteristics at low applied biases indicate the presence of conducting filaments in the active layer. The Ba device shows a high sharp onset in current at 2.2 V whereas the Al device shows a much weaker threshold. The inset shows the EL intensity from the two devices in arbitrary units; as shown, the limit of detection (L/O/D) coincides with the *x*-axis.

injection into the semiconductor is comparatively weak in this regime) and their presence gives rise to symmetric often nonlinear current-voltage characteristics.[16,17] The higher conductivity of the Al device in the low bias regime indicates that filament formation occurs more readily for Al than Ba. The formation of filaments, although widely evident in literature devices, is in general considered undesirable since it provides leakage pathways for injected carriers and is thought to accelerate device degradation through localized Joule heating. The erratic behavior of the current in the Al device between 3.6 and 5.4 V (which corresponds to genuine fluctuations in the circulating current rather than noise in the measurement system) is typical of systems with residual filamentary conduction, and is due to continual rupture and regeneration of the filaments at elevated drive voltages and temperatures. It should be stressed that the field-screening effects described below are not dependent on filament formation, and have also been observed in highly rectifying commercial devices that show no evidence of filament formation.[2–4]

The current through the Ba device increases sharply at 2.2 V followed by the onset of measurable electroluminescence at 3 V, indicating a transition to a regime in which charge transport occurs predominantly through the semiconductor rather than the filaments. The Al device has a much shallower current threshold and is significantly more resistive than the Ba device for biases above 2 V. As described above, due to the high barrier to hole injection, the efficiency of the Ba devices is expected to be low. In fact the measured external quantum efficiency Q of the Ba devices was unexpectedly high at around 0.8% ($\sim$3.5 cd/A) implying a surprisingly even balance of electron and hole injection despite the mismatched barrier heights. If as expected holes are the minority carrier, a lower limit for the hole injection current at the anode may be estimated from the EL efficiency and the measured current using Eq. (1),

$$Q = \gamma_{s-t} \times \phi_{\mathrm{fl}} \times \zeta_{\mathrm{out}} \times I_h/I \rightarrow I_h = \frac{QI}{\gamma_{s-t} \times \phi_{\mathrm{fl}} \times \zeta_{\mathrm{out}}}, \quad (1)$$

where γ_{s-t} is the singlet-triplet ratio, ϕ_{fl} is the fluorescence quantum efficiency of the composite film, ζ_{out} is the outcoupling efficiency of internally generated photons, I_h is the hole current at the anode, and I is the total current. The measured PL efficiency of 5BTF8, the singlet-triplet ratio and the outcoupling efficiency are all certainly less than 100% so from Eq. (1) the hole current at the anode must certainly be greater than $0.008I$. The total current density at 3.7 V is 5.72×10^{-3} A/cm^2, implying a minimum hole injection current density of 4.6×10^{-5} A/cm^2. This *hole* current is 35 times larger than the *total* current in the Al device (1.3×10^{-6} A/cm^2). Moreover, due to the losses associated with γ_{s-t}, ϕ_{fl}, ζ_{out}, the ratio of hole injection currents $I_h^{\mathrm{Ba}}/I_h^{\mathrm{Al}}$ in the two devices is likely to be substantially higher still. This is unexpected because the barrier to hole injection is the same for both devices but as we show later in Fig. 5, the Al device has a significantly lower flat-band bias of 1.8 V compared with 2.5 V for the Ba device. Therefore, at any given bias above 1.8 V, one would ordinarily expect stronger hole injection in the Al device due to the higher average field strength. It is therefore clear that the presence of electrons in the active layer leads to a substantial enhancement in the hole injection current. The same conclusion was drawn by Murata *et al.*[6] in their comparison of single- and double-carrier devices.

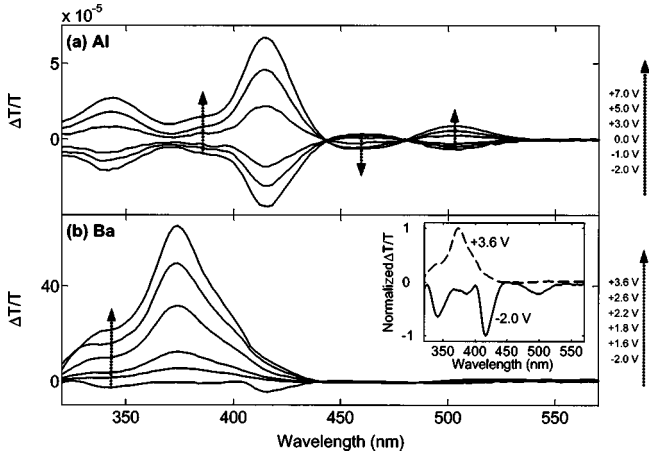

FIG. 3. First harmonic electromodulation spectra for the Al and Ba devices, using 1.4 V and 0.7 V RMS modulation biases respectively, and a variety of applied dc offsets. The EM spectrum of the Al device is dominated by the electroabsorption (EA) response of the polymer at all applied biases. The EM response of the Ba device is also dominated by electroabsorption in reverse bias but, when the device is operating in forward bias, the EA features are replaced by excited state bleaching and absorption due to injected charge.

Further insight into device operation can be obtained from EM spectroscopy which has been widely used to study internal electric fields in organic devices.[18–23] Figures 3(a) and 3(b) show for a variety of applied biases the first harmonic EM spectra for the Al and Ba devices, respectively. In a typical EM measurement, a combined ac and dc bias $V=V_{\mathrm{dc}}+V_{\mathrm{ac}}\sin(\omega t)$ is applied to the device, and changes in the transmission of a probe beam are monitored using phase sensitive lock-in detection. If the origin of the EM signal is electroabsorption (i.e., the Stark effect), the fractional change in transmission is proportional to the third order dc Kerr nonlinear susceptibility and the square of the electric field.[20] The differential transmission is therefore modulated at both the first and second harmonic frequencies in accordance with Eqs. (2a) and (2b),

$$I_\omega = \left.\frac{\Delta T}{T}\right|_\omega \propto 2\,\mathrm{Im}\,\chi^3(\lambda)E_{\mathrm{dc}}E_{\mathrm{ac}}\sin(\omega t), \quad (2a)$$

$$I_{2\omega} = \left.\frac{\Delta T}{T}\right|_{2\omega} \propto \frac{1}{2}\,\mathrm{Im}\,\chi^3(\lambda)E_{\mathrm{ac}}^2\cos(2\omega t). \quad (2b)$$

Under conditions of low carrier injection, the bulk field E_{dc} is related to the dc component of the applied voltage V_{dc} by $E_{\mathrm{dc}}=(V_{\mathrm{dc}}-V_{\mathrm{bi}})/d$, where V_{bi} is the built-in potential, and d is the width of the device. I_ω therefore varies linearly with V_{dc} (passing through zero at $V=V_{\mathrm{bi}}$), and $I_{2\omega}$ is independent of V_{dc}; any deviations from this behavior indicate nonuniform internal fields arising from the presence of substantial charge

in the device. The measurement of electroabsorption spectra in operational LEDs is complicated by the presence of strong modulated electroluminescence (EL) that is typically several orders of magnitude larger than the EM signal. The data reported here were obtained using a double modulation technique previously reported by Pires *et al.*[24] In short, the probe beam was modulated at a frequency ω_{probe} and the applied bias was modulated at a lower frequency ω_{osc}. Two lock-in amplifiers were used, the first acting as a (low time-constant) prefilter tuned to ω_{probe} and the second locking into the ω_{osc} frequency component of the prefiltered signal. In this way it was possible to attenuate the EL signal below the noise-floor of the measurement, permitting EM signals as small as one part in 10^7 to be obtained even for highly emissive operational devices.

The Al device shows a number of oscillatory electromodulation features with peaks at 344, 415, 460, and 504 nm and nodes at 443 and 481 nm. These oscillatory features are typical of electroabsorption, and this assignment is confirmed by the observations (not shown) that the spectra scale linearly with the dc bias and quadratically with the ac bias, as expected from Eqs. (2a) and (2b). The behavior of the Ba device however is more complex. The reverse bias EM spectrum shows equivalent peaks (344, 415, 460, and 504 nm) and nodes (443 and 481 nm), which also vary linearly with dc bias and exhibit a quadratic dependence on the ac bias, indicative of electroabsorption. However, these features are absent above 2.5 V and are replaced instead by a peak centered at 375 nm with shoulders at 335 and 400 nm. (The inset shows normalized spectra at −2.0 V reverse bias and +3.6 V forward bias for ease of comparison.) These features grow superlinearly with dc bias (and show a complex nonquadratic dependence on the ac bias) but do not otherwise change shape as the bias is increased. The absence of the EA features observed in reverse bias and the anomalous bias dependence of the spectral features indicates that the forward bias spectrum cannot be due to electroabsorption but must arise from another effect. The most probable cause, as described in previous manuscripts,[2–4] is modulation due to the injected charge, referred to here as excited state bleaching and absorption (ESBA). The response times of most organic LEDs are less than 1 μs (Ref. 25) and therefore for modulation frequencies below 1 MHz the injected charge is expected to follow the bias modulation, resulting in an EM signal that is independent of the modulation frequency. The data in Fig. 4(b) however reveals a strong reduction in the ESBA signal with increasing frequency, indicating a widening phase-lag between the current and the sinusoidal bias as the ac drive frequency is raised. The observed frequency dependence is broadly consistent with the dynamics of trapped charge, for which the in-phase and quadrature ESBA signals are related to the excitation lifetime τ and the modulation frequency ω by Eqs. (3a) and (3b)[26]

$$\Delta T(\omega)\Big|_x \propto \frac{1}{1+(\omega\tau)^2}, \tag{3a}$$

$$\Delta T(\omega)\Big|_y \propto \frac{\omega\tau}{1+(\omega\tau)^2}. \tag{3b}$$

We therefore attribute the ESBA signal of the Ba device in forward bias to trapped, as opposed to free, injected charge.

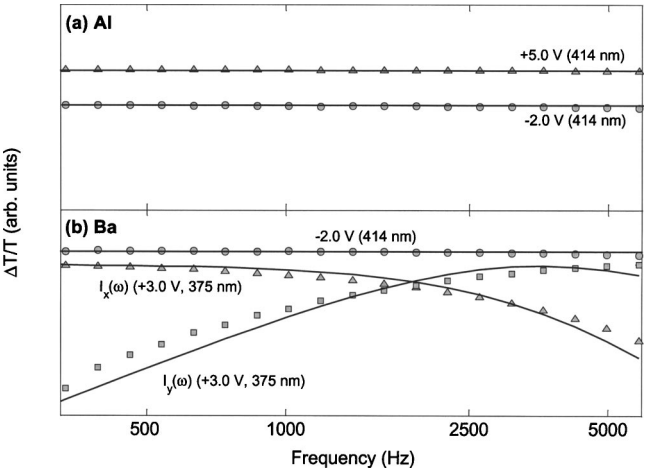

FIG. 4. The frequency dependence of the EM signals for (a) Al and (b) Ba devices. The EM response of the Al device, measured at 414 nm, shows no frequency dependence in the range 0.1–5 kHz in either reverse (circles) or forward (triangles) bias, indicating a fast response that is consistent with electroabsorption. The EM response of the Ba device in reverse bias is also consistent with EA (circles) but the forward bias EM signal measured at 375 nm (triangles, squares) shows a strong frequency dependence which fits well to a monomolecular decay of lifetime 41 μs and is consistent with trapped charge. The curves labeled $I_x(\omega)$ and $I_y(\omega)$ correspond respectively to the in-phase and quadrature components of the forward bias EM response of the Ba device.

The calculated lifetime of the trapped charge is 41 ± 0.5 μs. (The spectral features observed in the reverse bias EM spectrum of the Ba device and in the reverse and forward bias spectra of the Al device were found to be independent of modulation frequency consistent with the near-instantaneous response expected for electroabsorption, see Fig. 4.)

The EM response of the Ba device is typical of many polyfluorene-based LEDs containing PEDOT:PSS as we have reported in previous manuscripts.[2–4] The complete suppression of the field-induced spectral features above turn-on indicates that the internal field is screened by the injected charge as has been previously explained in Refs. 2–4. In order to screen the bulk semiconductor from the external field, the injected charges must accumulate at the counter electrode,[27] causing a substantial enhancement of the local electric field and leaving the bulk semiconductor largely field-free. The observed field screening is therefore due to either trapped electrons at the anode or trapped holes at the cathode. The absence of comparable effects in the Al device indicates that electrons are responsible for the screening, giving rise to the situation illustrated in Fig. 1(a). This conclusion is further supported by the observed current-voltage-luminance characteristics since the enhanced local field at the anode will increase the rate of (field-dependent) hole injection, leading to a better balance of electron and hole injection (and hence higher EL efficiencies) than would otherwise occur, as seen in Fig. 2.

In Fig. 5 we show the dc bias dependence of the first harmonic electroabsorption response for (i) the Al device and (ii) the Ba device. The first harmonic response of the Al device varies linearly with applied bias in accordance with

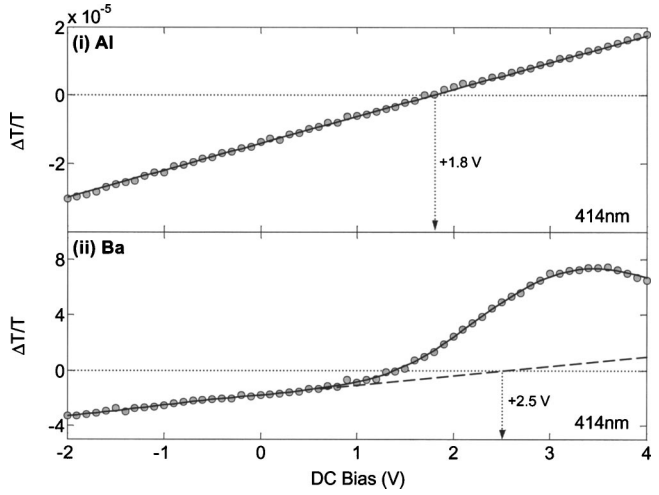

FIG. 5. The dc bias dependence of the first harmonic electromodulation signal at 414 nm for (i) Al and (ii) Ba devices; the dashed line indicates the expected signal in the absence of field redistribution.

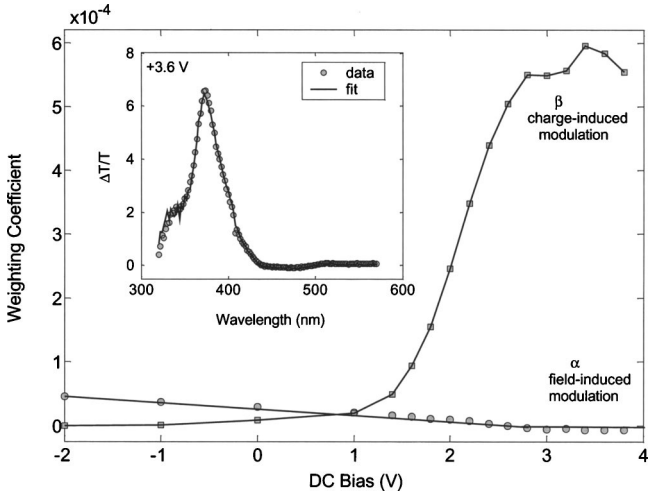

FIG. 6. The variation of the weighting coefficients α and β with applied dc bias, where α indicates the field-induced modulation and β indicates the charge-induced modulation. Above 2.6 V, α is approximately zero, indicating suppression of the electric field. The inset shows a typical fit to Eq. (4) obtained at 3.6 V.

Eq. (2a) indicating a linear variation of bulk field with applied bias. The first harmonic response of the Ba device, however, shows a linear variation with dc bias only in the range −2 to +1 V; at higher biases the signal deviates significantly from the linear (dotted line) when charge-induced modulation becomes important.

The loss of EA signal in the Ba device suggests that the internal field is screened above the turn-on bias, as we have previously reported for other devices containing PEDOT:PSS. In earlier manuscripts, we were able to test this hypothesis by identifying spectral regions in which, the measured EM signal was due entirely to the Stark effect, with negligible contamination from charge-induced modulation. Hence, by monitoring the dc bias dependence of the EM signal at these "SE-only" wavelengths, we were able to show that the field-induced modulation signal fell to zero above turn-on, indicating full screening of the internal field. The charge-induced spectral features of the devices reported here, however, overlap strongly with the dominant electroabsorption features, making an equivalent analysis difficult. In order to analyze the relative importance of field- and charge-induced modulation in these devices we instead make the crude assumption that the measured first harmonic EM spectrum $I_\omega(\lambda, V)$ at an applied bias V may be expressed as a simple linear superposition of two bias-independent spectra

$$I_\omega(\lambda, V) = \alpha(V)F(\lambda) + \beta(V)C(\lambda), \tag{4}$$

where α and β are bias-dependent weighting coefficients, and $F(\lambda)$ and $C(\lambda)$ are the field- and charge-induced modulation spectra, respectively. We are interested in determining how α and β depend on the applied bias, and this may be straightforwardly determined by fitting the electromodulation spectra in Fig. 3 to Eq. (4) using least squares optimization. To do so, it is necessary first to select suitable spectra for $F(\lambda)$ and $C(\lambda)$. $F(\lambda)$ was arbitrarily set equal to the measured modulation spectrum at −2 V, since the spectral features in reverse bias are known to correspond to electroabsorption. $C(\lambda)$ was set equal to $I_\omega(\lambda, 2.6)$, the modulation spectrum measured close to the flat-band voltage, at which bias the field-induced contributions are negligible.[28] However, since the shapes of the forward- and reverse-bias spectra are not found to vary substantially with bias, it does not greatly matter which spectra are selected for $F(\lambda)$ and $C(\lambda)$, as long as they are, respectively, drawn from measurements that are taken well into reverse and forward bias. The results of the fitting procedure are shown in Fig. 6. The inset shows a typical fit to Eq. (4) obtained at 3.6 V. α, the field-related coefficient, decreases linearly with dc offset until reaching zero at 2.6 V. This behavior is expected and indicates a linear decrease in the bulk field with increasing applied bias until the flat-band condition is reached. α does not however subsequently rise in magnitude as would be expected for the formation of a forward biased electric field in the device (dotted line) but instead it remains close to zero indicating neutralisation of the internal field. The charge-related coefficient β increases rapidly with dc-offset reflecting the rapid increase in carrier injection (and the consequent increase in the population of trap sites). The behavior of α and β is consistent with previous measurements using materials with spectral regions in which the measured EM signal was due entirely to the Stark effect.

III. CONCLUSION

In conclusion, we have fabricated ITO/PEDOT:PSS/5BTF8/metal devices, where the top metallic electrode is chosen as either Ba or Al to provide, respectively, efficient or inefficient electron injection. The Al devices exhibit low currents, indicating low rates of electron and hole injection, whereas the Ba devices exhibit high currents and high electroluminescence efficiencies, implying efficient injection of both electrons *and* holes despite sizable hole injection barriers of 0.7 ± 0.1 eV. The Al devices exhibit conventional field-

induced EM behavior consistent with the Stark effect. The Ba devices show conventional SE behavior for low applied biases but, above turn-on, the SE features vanish due to screening of the internal field, and are replaced by charge-induced bleaching and absorption features. The behavior of the devices is consistent with the presence of electron traps close to the PEDOT:PSS/organic interface. Al electrodes provide poor electron injection, which leaves the traps unpopulated and the bulk field unaffected. Ba electrodes provide efficient electron injection, which populates the trap-sites, causing the potential to drop preferentially at the PEDOT:PSS/organic interface and reducing the magnitude of the bulk field [Fig. 1(a)]. The high field-strength at the anode increases the rate of field-dependent hole injection, leading to improved balance of injection rates for electrons and holes and higher device efficiencies. The findings are consistent with complementary studies by Murata *et al.*,[6] Van Woudenbergh *et al.*,[7,10] and Poplavskyy *et al.*[8,9] Finally, we note that, to date, we have only observed screening in polyfluorene based devices that also contain PEDOT:PSS, and the potential role of PEDOT:PSS in trap formation is a subject that will be addressed in a future manuscript.

ACKNOWLEDGMENTS

We are grateful for financial support from the UK Engineering and Physical Sciences Research Council (GR/S96791/01).

*Author to whom correspondence should be addressed. Electronic mail: j.demello@imperial.ac.uk

[1] R. H. Friend, R. W. Gymer, A. B. Holmes, J. H. Burroughes, R. N. Marks, C. Taliani, D. D. C. Bradley, D. A. D. Santos, J. L. Brédas, M. Lögdlund, and W. R. Salaneck, Nature (London) **397**, 121 (1999).

[2] P. A. Lane, J. C. deMello, R. B. Fletcher, and M. Bemius, Appl. Phys. Lett. **83**, 3611 (2003).

[3] P. A. Lane, J. C. deMello, R. B. Fletcher, and M. T. Bemius, Proc. SPIE **5214**, 162 (2004).

[4] P. J. Brewer, P. A. Lane, A. J. deMello, D. D. C. Bradley, and J. C. deMello, Adv. Funct. Mater. **14**, 562 (2004).

[5] J. C. deMello, N. Tessler, S. C. Graham, and R. H. Friend, Phys. Rev. B **57**, 12951 (1998).

[6] K. Murata, S. Cina, and N. C. Greenham, Appl. Phys. Lett. **79**, 1193 (2001).

[7] T. V. Woudenbergh, P. W. M. Blom, and J. N. Huiberts, Appl. Phys. Lett. **82**, 985 (2003).

[8] D. Poplavskyy, J. Nelson, and D. D. C. Bradley, Appl. Phys. Lett. **83**, 707 (2003).

[9] D. Poplavskyy, J. Nelson, and D. D. C. Bradley, Proc. SPIE **5214**, 197 (2004).

[10] T. V. Woudenbergh, J. Wildeman, P. W. M. Blom, J. J. A. M. Bastiaansen, and B. M. W. Langeveld-Voss, Adv. Funct. Mater. **14**, 679 (2004).

[11] As discussed in Ref. 4, there was some indirect evidence concerning the role of electrons: first a degree of partial field-redistribution was evident in the electron-only bias regime below turn-on and, second, screening effects were observed only in devices containing PEDOT:PSS. This latter issue will be investigated in more detail in a later manuscript.

[12] R. B. Fletcher, D. G. Lidzey, D. D. C. Bradley, M. Bemius, and S. Walker, Appl. Phys. Lett. **77**, 1262 (2000).

[13] A. J. Campbell, D. D. C. Bradley, and H. Antoniadis, J. Appl. Phys. **89**, 3343 (2000).

[14] R. Pacios and D. D. C. Bradley, Synth. Met. **127**, 261 (2002).

[15] Ba may also form an Ohmic contact with PFO but, given the experimental uncertainty in the quoted values for energy levels and work functions, a small barrier may possibly exist.

[16] R. D. Gould, J. Non-Cryst. Solids **55**, 363 (1983).

[17] S. Gravano, E. Amr, R. D. Gould, and M. A. Samra, Thin Solid Films **433**, 321 (2003).

[18] J. C. deMello, J. J. M. Halls, S. C. Graham, N. Tessler, and R. H. Friend, Phys. Rev. Lett. **85**, 421 (2000).

[19] C. Giebeler, S. A. Whitelegg, A. J. Campbell, M. Liess, S. J. Martin, P. A. Lane, D. D. C. Bradley, G. Webster, and P. L. Burn, Appl. Phys. Lett. **74**, 3714 (1999).

[20] I. H. Campbell, T. W. Hagler, D. L. Smith, and J. P. Ferraris, Phys. Rev. Lett. **76**, 1900 (1996).

[21] P. A. Lane, J. Rostalski, C. Giebeler, S. J. Martin, D. D. C. Bradley, and D. Meissner, Sol. Energy Mater. Sol. Cells **63**, 3 (2000).

[22] S. J. Martin, G. L. B. Verschoor, M. A. Webster, and A. B. Walker, Org. Electron. **3**, 129 (2002).

[23] I. Hiromitsu, Y. Murakami, and T. Ito, J. Appl. Phys. **94**, 2434 (2003).

[24] M. P. Pires, P. L. Souza, and J. P. V. d. Weid, Braz. J. Phys. **26**, 252 (1996).

[25] D. J. Pinner, R. H. Friend, and N. Tessler, J. Appl. Phys. **86**, 5116 (1999).

[26] E. Ehrenfreund, O. Epshtein, Y. Eichen, M. Wohlgenannt, and Z. V. Vardeny, Synth. Met. **137**, 1363 (2003).

[27] The accumulation of electrons or holes close to the parent electrode would increase the bulk field as seen for example in space-charge limited devices.

[28] The flat band bias may be determined by extrapolation of the linear regime of Fig. 5(ii) to zero, yielding a value of 2.5 V.

[29] D. R. Lide, *Handbook of Chemistry and Physics*, 85th ed. (CRC Press, Boca Raton2004–2005).

[30] N. Koch, A. Kahn, J. Ghijsen, J.-J. Pireaux, J. Schwartz, R. L. Johnson, and A. Eischner, Appl. Phys. Lett. **82**, 70 (2003).